Polymer Journal (2016) 48, 421–429

www.nature.com/pj

ORIGINAL ARTICLE

Conjugated fluorene-moiety-containing pendant polymers for the dispersion of single-wall carbon nanotubes: polymer wrapping abilities and electrical properties

Hsuan-Chun Chang[1,3], Jau-Tzeng Wang[1,3], Dian-Han Li[1], Chien Lu[1], Han-Wen Hsu[2], Hung-Chin Wu[1], Cheng-Liang Liu[2] and Wen-Chang Chen[1]

We report a new strategy to disperse single-wall carbon nanotubes (SWNTs) via conjugated moiety-containing pendant polymers, poly(2-vinylpyridine)-*co*-poly(9,9-dihexyl-2-(4-vinylphenyl)-9*H*-fluorene) (P2VP-*co*-P(StFl)). The polymer composition ratio and molecular weight were varied to control the SWNT dispersion. The P(St-Fl) segments were adsorbed to the surface of the de-bundled SWNTs through π–π interaction, while the P2VP segments surrounded the outer surfaces of the SWNTs to enhance their solubility and stability. A low-voltage field-effect transistor (FET) was fabricated using a P(St-Fl)-wrapped SWNT network, SWNTs wrapped with $P2VP_{79}$-*co*-$P(St\text{-}Fl)_{347}$, and hafnium oxide as the active layer, gate electrode, and dielectric, respectively. The field-effect mobility of the fabricated device was as high as 0.82 $cm^2 V^{-1} s^{-1}$ on average, with an ON/OFF ratio over 10^4 under a −5 V bias. This study highlights the tailored wrapping power of pendant polymers, as well as the tunable electrical conducting/semiconducting properties of SWNTs for FET device applications.
Polymer Journal (2016) **48,** 421–429; doi:10.1038/pj.2015.122; published online 13 January 2016

INTRODUCTION

Single-wall carbon nanotubes (SWNTs) are ideal components for flexible and low-power electronic devices due to their superior electrical and mechanical properties, as well as their environmental stability.[1–4] Their excellent quasi-one-dimensional charge transport properties have attracted tremendous scientific interest, and they have been studied for applications relating to display drivers, photovoltaics, and circuits.[5–7] In addition, the extreme environmental sensitivity of SWNTs makes them ideal active components for biological and chemical sensors[8–10] because their charge transport properties are directly influenced by molecular adsorbents. However, the homogenous dispersion of SWNTs remains a challenge for device-related applications.

Among the numerous approaches developed to disperse SWNTs,[11–13] polymer-assisted dispersion in non-aqueous solvents by non-covalent attachments represents one of the most effective separation methods due to its high effectiveness and scalability.[14–16] Recently, three approaches to the use of polymeric materials as dispersants have received significant attention. The first approach is the functionalization of SWNTs with conjugated aromatic polymers/oligomers, such as poly(m-phenylene vinylene),[17,18] poly(3-alkylthiophene),[19–21] and poly(9,9-dioctylfluorene).[22–27] The π-conjugated backbone of the conjugated polymer interacts with the π-electron surface of the nanotube to support their debundling and dispersion. However, the resulting dispersions have limited solubility and stability because the hydrophobic main-chain conjugated rods themselves face inherent overall solubility issues due to the formation of strong π–π stacking interactions. The second approach is the use of block copolymers,[28] which provide stable dispersions of physically adsorbed individual SWNTs and permit manipulating the solubility of the carbon nanotubes by the composition of the block copolymers. To this end, the conjugated block copolymers are designed as efficient dispersant agents such that the conjugated block strongly adheres to the carbon nanotube wall surface, while the other mechanically flexible block provides solubility for the exfoliated nanotubes by forming a steric barrier and producing a repulsion interaction between the polymer-wrapped nanotubes.[29–33] For example, conjugated rod-coil copolymers including poly(3-hexylthiophene) (P3HT)-*b*-poly(methyl methacrylate),[29] P3HT-*b*-poly(acrylic acid),[29] P3HT-*b*-poly(poly (ethylene glycol) methyl ether acrylate)[29] and P3HT-*b*-polystyrene have been employed for SWNTs dispersion.[30] In the third approach, vinyl polymers containing side-chain pyrene groups have been non-covalently bonded with SWNTs.[34–37] The introduction of π–π interactions by using a copolymer with pendant conjugated moieties is a

[1]Department of Chemical Engineering, National Taiwan University, Taipei, Taiwan and [2]Department of Chemical and Materials Engineering, National Central University, Taoyuan, Taiwan
[3]These two authors contributed equally to this work.
Correspondence: Professor W-C Chen, Department of Chemical Engineering, National Taiwan University, Taipei, 10617, Taiwan.
E-mail: chenwc@ntu.edu.tw
Received 14 October 2015; revised 13 November 2015; accepted 15 November 2015; published online 13 January 2016

promising strategy to disperse SWNTs.[38–40] A main-chain flexible backbone combined with side-chain conjugated moieties can effectively wrap around SWNTs to make them dispersible in solvents. However, the identification of pendant polymers with specific conjugated moieties for the preferential dispersion of SWNTs has not yet been fully explored, and the tunable polymer wrapping power required to precisely control the electrical properties of SWNTs is not yet fully understood.

In this study, different compositions of pendant fluorene-based poly(2-vinylpyridine)-*co*-poly(9,9-dihexyl-2-(4-vinylphenyl)-9*H*-fluorene) (P2VP-*co*-P(St-Fl)) copolymers and the corresponding P2VP and P(St-Fl) homopolymers were synthesized to evaluate the ability of these polymers to disperse SWNTs. The pendant conjugated fluorene moieties in P(St-Fl) segment could adhere to the SWNT surface through π–π interactions because of the isomorphic molecular skeleton on the nanotube surface,[22–24] while the P2VP segment provided the flexibility needed to improve solubility. A detailed schematic illustration of the SWNTs field-effect transistor (FET) fabrication procedure is provided in Figure 1. The pendant-polymer-wrapped SWNTs were spray coated onto the glass substrate. After the removal of the polymer matrix at a higher temperature, distinctive conducting and semiconducting channel characteristics could be observed, depending on the SWNTs density on the solid substrate. The solution-phase processing of a SWNT random-network-based FET with a SWNT gate electrode was realized with a reasonable mobility and a high ON/OFF ratio. Our results demonstrate how conjugated fluorene-moiety-containing pendant polymers can be used to disperse SWNTs in the wrapping mode and precisely control the SWNTs density to study the electrical properties of the FET device.

EXPERIMENTAL PROCEDURE

Materials

All the reagents and solvents were purchased from Aldrich (St Louis, MO, USA) and TCI (Tokyo, Japan) unless stated otherwise. 2-Vinylpyridine was distillated from CaH_2 powder and dibutyl magnesium (1 M in heptane) under reduced pressure before use. P(St-Fl) homopolymer was synthesized via living anionic polymerization, as reported in our previous works.[41,42] All the detailed synthetic routes for pendant polymers are shown in Scheme 1.

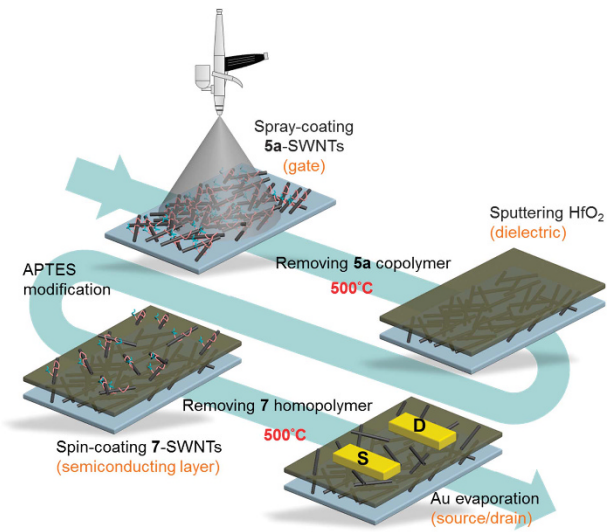

Figure 1 Schematic illustration of the single-wall carbon nanotubes (SWNT) field-effect transistor (FET) fabrication procedure.

Synthesis of poly(2-vinylpyridine) macroinitiator (P2VP-Br, 3a and 3b)

CuBr (44.5 mg, 0.31 mmol) and Me4cyclam (81.6 mg, 0.32 mmol) were added to a Schlenk flask, and the flask was evacuated and backfilled with nitrogen three times. Then, degassed 2-vinylpyridine (5 ml, 46.4 mmol), methyl 2-bromopropionate (35 µl, 0.31 mmol) and anisole (4 ml) were added, and the mixture was stirred for 30 min to produce the CuBr/Me4cyclam complexes. Then, the reaction flask was immersed in an oil bath at 90 °C and stirred for 24 h. The polymerization was quenched by exposure to air. After cooling to room temperature, the viscous polymer solution was diluted with tetrahydrofuran (THF), and the copper residue was removed by passing the liquid mixture through a neutral Al_2O_3 column. The light-yellow filtrate was concentrated, re-precipitated from *n*-hexane, collected by filtration, and dried under vacuum to obtain the $P2VP_{79}$-Br (**3a**) product (yield: 23%; M_n = 8300 g mol^{-1}, polydispersity index (PDI) = 1.21). ^{1}Proton nuclear magnetic resonance (H NMR) ($CDCl_3$): δ(p.p.m.) = 8.4–8.0 (m, 1H), 7.3–7.0 (m, 1H), 7.0–6.7 (m, 1H), 6.5–6.2 (m, 1H), and 2.0–1.4 (broad, backbone). Using a similar procedure to that described above, the $P2VP_{140}$-Br (**3b**) product was obtained (yield: 35%; M_n = 14 700 g mol^{-1}, PDI = 1.31).

Synthesis of poly(2-vinylpyridine)-*co*-poly(4-bromostyrene) (P2VP-*co*-P(4BrSt)), 4a and 4b)

Typically, **3a** (605 mg, 0.041 mmol), CuBr (7.8 mg, 0.054 mmol), and Me4cyclam (15.6 mg, 0.061 mmol) were added to a Schlenk flask, and the flask was evacuated and backfilled with nitrogen three times. Then, degassed 4-bromostyrene (1.1 ml, 4.29 mmol) and anisole (4.5 ml) were added, and the mixture was stirred for 30 min to carry out the CuBr/Me4cyclam complexes. Subsequently, the reaction flask was immersed in an oil bath at 120 °C for 24 h. The polymerization was quenched by exposure to air. After cooling to room temperature, the viscous polymer solution was diluted with THF, and the copper species were removed by passing the liquid mixture through a neutral Al_2O_3 column. Then, it was precipitated into an excess of *n*-hexane, filtered out, and dried under vacuum at 40 °C to obtain $P2VP_{79}$-*co*-$P(4BrSt)_{347}$ (**4a**) as a white solid (yield: 48%; M_n = 71 800 g mol^{-1}, PDI = 1.35). ^{1}H NMR (CD_2Cl_2): δ(p.p.m.) = 8.4–8.0 (pyridine ring aromatic protons), 7.4–6.2 (broad, aromatic protons), and 2.0–1.5 (broad, backbone and C_6H_{13}). Using a similar procedure to that described above, $P2VP_{140}$-*co*-$P4BrSt_{15}$ (**4b**) was obtained (yield: 45%; M_n = 17 500 g mol^{-1}, PDI = 1.29).

Synthesis of poly(2-vinylpyridine)-*co*-poly(9,9-dihexyl-2-(4-vinylphenyl)-9H-fluorene) (P2VP-*co*-P(St-Fl), 5a and 5b)

A mixture of **4a** (290 mg, 0.017 mmol), 9,9-di-*n*-hexylfluorenyl-2-boronic acid (191 mg, 0.5 mmol), $Pd(PPh_3)_4$ (58.9 mg, 0.051 mmol) and five drops of Aliquat 336 was dissolved in anhydrous THF and 2 M Na_2CO_3 aqueous solution under reflux at 80 °C. The reaction flask was immersed in an oil bath at 85 °C, and the reaction mixture was vigorously stirred for 6 days. The polymer was purified by washing with acetone/DI water (1/1 vol) and finally freeze-dried from its benzene solution to obtain the yellow solid of $P2VP_{79}$-*co*-$P(St\text{-}Fl)_{347}$ (**5a**) (yields: 19%; M_n = 159 800 g mol^{-1}, PDI = 1.55). ^{1}H NMR (CD_2Cl_2): δ(p.p.m.) = 7.7–6.2 (broad, aromatic protons), 2.2–0.6 (broad, backbone, and C_6H_{13}). Using a similar procedure to that described above, $P2VP_{140}$-*co*-$P(St\text{-}Fl)_{15}$ (**5b**) was obtained (yield: 23%; M_n = 21 200 g mol^{-1}, PDI = 1.33).

Synthesis of poly(4-bromostyrene) macroinitiator (P(4BrSt)-Br, 6)

CuBr (22.3 mg, 0.15 mmol) and Me4cyclam (40.8 mg, 0.16 mmol) were added to a Schlenk flask, which was evacuated and backfilled with nitrogen three times. Degassed 4-bromostyrene (10.46 ml, 80 mmol), which was first passed through a column filled with basic alumina to remove the inhibitor; methyl 2-bromopropionate (17.5 µl, 0.15 mmol); and anisole (8 ml) were added via a degassed syringe, and the mixture was stirred for 30 min to produce the CuBr/Me4cyclam complexes. Then, the reaction flask was immersed in an oil bath at 90 °C and stirred overnight. The polymerization was stopped by opening the flask and exposing the catalyst to air. After cooling to room temperature, the viscous polymer solution was diluted with a small amount of THF and purified by passing through a column filled with neutral alumina to

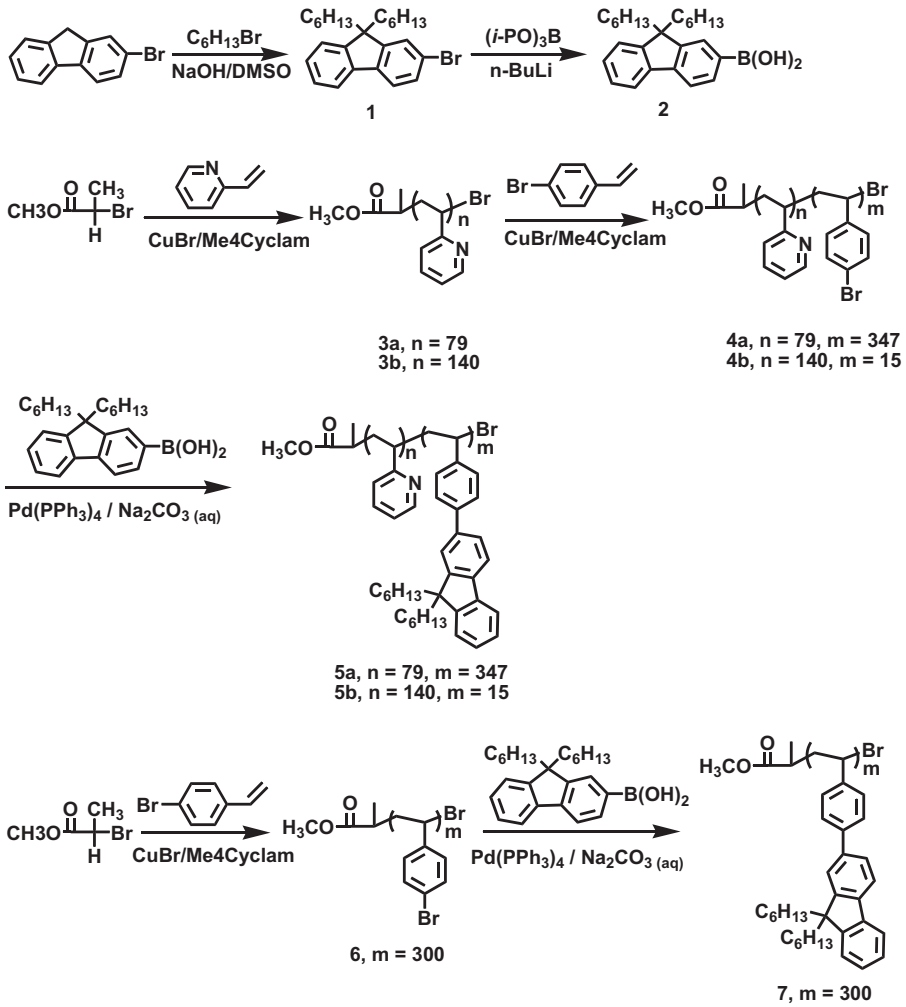

Scheme 1 Synthesis of the P2VP-*co*-P(St-Fl) (**5**) copolymers and $P(St\text{-}Fl)_{300}$ (**7**) homopolymer.

remove the copper complex. The eluent was precipitated by pouring the solution into a large excess of *n*-hexane to obtain **6** (yield: 43%; $M_n = 55\,000\ g\ mol^{-1}$, PDI = 1.37). ^1H NMR (CD_2Cl_2): δ(p.p.m.) = 7.4–6.8 (m, 2H), 6.5–6.2 (m, 2H), and 2.0–1.4 (broad, backbone).

Synthesis of poly(9,9-dihexyl-2-(4-vinylphenyl)-9H-fluorene) ($P(St\text{-}Fl)_{300}$, 7)

A mixture of **6** (550 mg, 0.01 mmol), 9,9-di-*n*-hexylfluorenyl-2-boronic acid (191 mg, 0.5 mmol), $Pd(PPh_3)_4$ (58.9 mg, 0.051 mmol) and five drops of Aliquat 336 was dissolved in anhydrous THF and 2.0 M Na_2CO_3 aqueous solution under reflux. The reaction flask was immersed in an oil bath at 85 °C, and the reaction mixture was vigorously stirred for 6 days. The polymer was purified by washing with acetone/deionized water (1/1 volume ratio), acetone, *n*-hexane, and diethyl ether. Finally, the polymer was freeze-dried from benzene solution to obtain the $P(St\text{-}Fl)_{300}$ (**7**) yellow solid (yields: 39%; $M_n = 119\,000\ g\ mol^{-1}$, PDI = 1.43). ^1H NMR (CD_2Cl_2): δ(p.p.m.) = 7.7–6.2 (broad, aromatic protons) and 2.2–0.6 (broad, backbone, and C_6H_{13}).

Characterization

The molecular weight distribution was determined by gel permeation chromatography (GPC) using a Lab Alliance RI2000 instrument (PLgel 5 μm MIXED-D from Polymer Laboratories; Laballiance Instrument Co., Beijing, China) connected to a refractive index detector from Schambeck SFD Gmbh. All GPC analyses were performed on a polymer/toluene solution at a flow rate of 1 ml min^{-1} at 60 °C and calibrated with polystyrene. The morphology of polymer film surface was obtained with a Nanoscope 3D Controller atomic force microscopy (AFM, Digital Instruments, Santa Barbara, CA, USA). ^1H NMR spectra were recorded at room temperature on a Bruker AM 500 (500 MHz) spectrometer using the residual proton resonance of deuterated chloroform as the internal standard. Thermal analyses were performed on a differential scanning calorimetry from TA Instruments (TA Q100, TA Instruments Inc., New Castle, DE, USA) with a heating cycle from − 10 to 200 °C at a heating rate of 10 °C min^{-1} and a thermal gravimetric analyzer from Perkin-Elmer 7 over a heating range from 95 to 800 °C at a heating rate of 20 °C min^{-1}. UV–vis optical absorption and photoluminescence (PL) spectra were recorded using a Hitachi U-4100 spectrometer (Hitachi High-Technologies Corporation, Tokyo, Japan) and a Jobin Yvon Fluorolog-3 spectrofluorometer (Horiba Scientific, Edison, NJ, USA), respectively. Raman spectroscopy (Jobin Yvon LabRAM HR800) was performed using a He-Ne laser at a wavelength of 632.8 nm.

Preparation of polymer/SWNT solution

The synthesized polymers were dissolved in toluene at a concentration of 6 mg ml^{-1}. Subsequently, SWNTs (2 mg; Sigma-Aldrich) were added to the polymer solution. The solution was then sonicated with an ultrasonic liquid processor (Sonicator 3000, QSonica, Newtown, CT, USA) for 1 h at 70 W. Following this stage, the dispersions were centrifuged with an Optima XE-90 instrument (Beckman Coulter, Brea, CA, USA; SW55 Ti Rotor) at 40 000 r.p.m. for 30 min, and only the upper supernatant of the centrifuged material was included to remove large bundles and carbon contaminants, as well as to enrich the SWNT solution.

Fabrication of SWNT FET

A detailed schematic illustration of the SWNT FET fabrication procedure is provided in Figure 1. The suspension of SWNTs wrapped with **5a** was spray-coated on the glass substrate. The nozzle-to-substrate surface distance was fixed at 10 cm, and the spray time was 60 s to control the quality and density of SWNTs in the composite film. HfO_2 was deposited as the gate dielectric layer by the RF-sputtering method. Then, the HfO_2/glass substrate was treated with ozone plasma for 5 min. An active layer of SWNTs wrapped with **7** was obtained by spin-coating at 4000 r.p.m. onto the 3-aminopropyl-triethoxysilane-modified HfO_2 substrate. Note that it was necessary to treat the devices at a high temperature of >500 °C to remove all **5a** and **7** polymers. Finally, gold source/drain electrodes (30 nm) were formed by thermal evaporation through a regular shadow mask with a channel length (L) and width (W) of 50 and 1000 μm, respectively. The electrical characteristics of the SWNT FET were determined out using a Keithley 4200-SCS semiconductor parametric analyzer (Keithley Instruments Inc., Cleveland, OH, USA) at room temperature in a N_2-filled glove box. At least 10 testing cells per device were characterized to assess the reproducibility.

RESULTS AND DISCUSSION

Polymer synthesis and characterization

The structures of the pendant polymers were characterized by NMR and GPC. Figure 2 shows the ^{1}H NMR spectra of $P2VP_{79}$-Br (**3a**), $P2VP_{79}$-*co*-$P(4BrSt)_{347}$ (**4a**), and $P2VP_{79}$-*co*-$P(St\text{-}Fl)_{347}$ (**5a**) in CD_2Cl_2. The characteristic proton resonance signals from the pyridinyl and -CCH_2- are clearly observed at 8.4 − 8.0, 7.3 − 7.0, 7.0–6.7, 6.5–6.2 and 2.0–1.4 p.p.m. in Figure 2a. By the GPC analysis shown in Supplementary Figure S1, the molecular weight (M_n) and PDI of the P2VP are estimated to be 8300 g mol^{-1} and 1.21, respectively, from which the repeat unit number of P2VP is estimated to be 79. Figure 2b shows the ^{1}H NMR spectrum of **4a** copolymers in CD_2Cl_2. The proton peaks located at 8.4–8.0 and 7.1–6.8 p.p.m. are assigned to pyridinyl, and those at 7.6–7.2 and 6.7–6.2 p.p.m. are attributed to the aromatic ring of P(4BrSt). The M_n and PDI of **4a** estimated from the GPC curve are 71 800 g mol^{-1} and 1.35, respectively, from which the monomer repeat unit number of P(4BrSt) is estimated to be 347. The ^{1}H NMR spectrum of **5a** is shown in Figure 2c. A broad peak is clearly observed from 7.7 to 6.2 p.p.m. due to the attached fluorene block. In addition, the M_n and PDI of **5a** estimated from GPC are 159 830 g mol^{-1} and 1.55, respectively, which clearly shifts to the high-molecular-weight region without significant tailing at the lower-molecular-weight region (Supplementary Figure S1). This result demonstrates that most of P(4BrSt) segments are converted to P(St-Fl) during the Suzuki coupling reaction in the side group. Similarly, $P2VP_{140}$-*co*-$P(St\text{-}Fl)_{15}$ (**5b**), P(4BrSt)-Br (**6**), and $P(St\text{-}Fl)_{300}$ (**7**) were also well-characterized by ^{1}H NMR and GPC, as shown in Supplementary Figures S2–S4. The M_n and PDI of all the synthesized pendant polymers are summarized in Table 1. Thermal properties of the studied polymers were examined by thermal gravimetric analyzer and differential scanning calorimetry. The thermal gravimetric analyzer curves of **5a**, **5b**, and **7** exhibit the thermal degradation temperatures (T_d; weight loss of 10%) at 360, 435 and 305 °C, respectively, as shown in Supplementary Figure S5. The glass transition temperatures (T_g) of the **5a**, **5b,** and **7** obtained from the differential scanning calorimetry curves in Supplementary Figure S6 are found at 88, 105, and 83 °C, respectively. The T_g of **5b** is close to that of the P2VP homopolymer (97 °C) because the molecular weight of the P2VP block is much larger than that of the P(St-Fl) block. Simultaneously, the T_g of **5a** is closer to that of **7** (83 °C).

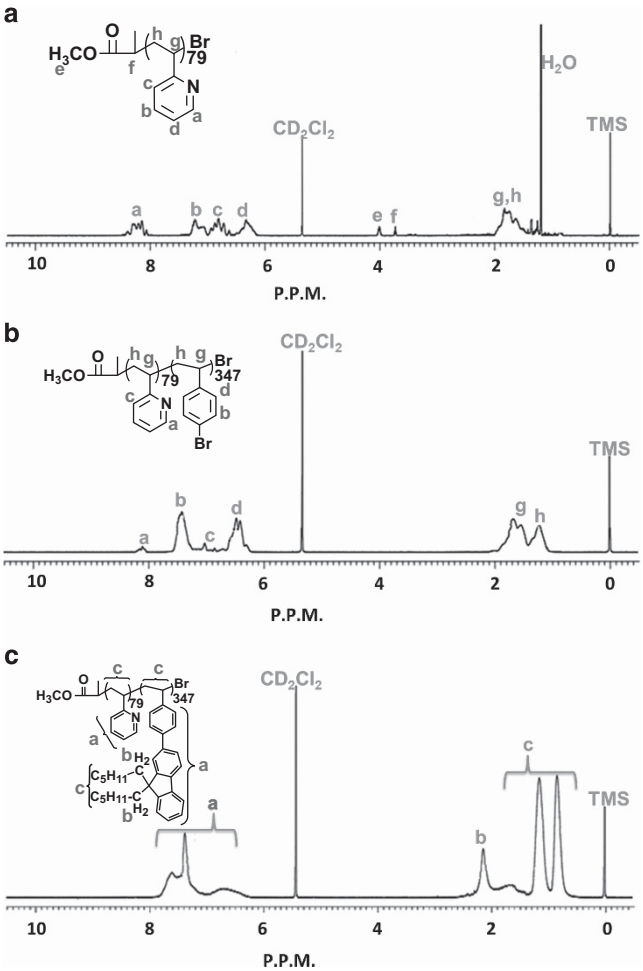

Figure 2 1H NMR spectra of (**a**) **3a**, (**b**) **4a**, and (**c**) **5a** in CD_2Cl_2. A full color version of this figure is available at the *Polymer Journal* online.

Dispersion of pendant-polymer-wrapped SWNTs

Commercial arc-discharge nanotubes (diameter: 1–2 nm, length: 1–3 μm), which are known to have superior conductivity in networks compared with tubes synthesized by other methods,[43] were used in this study. All the studied pendant polymers, $P2VP_{79}$-*co*-$P(St\text{-}Fl)_{347}$ (**5a**), $P2VP_{140}$-*co*-$P(St\text{-}Fl)_{15}$ (**5b**), $P(St\text{-}Fl)_{300}$ (**7**), P2VP, and $P(St\text{-}Fl)_{29}$, were designed for comparison of their wrapping capability in solution, as illustrated in Supplementary Figure S7. To disperse the SWNTs, an initial polymer:SWNT weight ratio of ~3:1 was blended in toluene. Sonication was then used to increase the uniformity of the composite suspensions and induce interaction between the polymer and SWNTs. The sonication power (<70 W) and time (<60 min) were limited to minimize tube damage and cutting. After the sonication process, centrifugation was performed to remove bundles and carbon contaminants and to enrich the SWNT solution. An obvious brown color was observed in the **5a**/ and **7**/SWNT mixtures (Figures 3a and b) after centrifugation, indicating that many SWNTs were successfully wrapped by the conjugated fluorene-containing pendant polymers. A large quantity of the highly concentrated SWNT suspension could be obtained by dispersing SWNTs in **7** (20–23 μg ml^{-1}) and **5a** (30–35 μg ml^{-1}) polymer solution (Figures 3a and b). The effect of the block ratio of the pendant copolymers on the dispersion of the polymer-wrapped SWNTs was also determined. Specifically, the molecular weight of the polymer block with the side-chain-conjugated fluorene moieties has a significant impact. Here, the mixtures of P2VP/, $P(StFl)_{29}$/ and **5b**/SWNTs seem to be clear after the sonication and centrifugation processes (Figures 3c–e). The poor

Table 1 Characterization of synthesized comb-like polymers and their SWNTs wrapping density

Polymer	M_n[a] *(P2VP) (gmol^{-1})*	M_n[a] *(P(St-FI)) (gmol^{-1})*	*PDI*[a] *(—)*	T_d[b] *(°C)*	T_g *(°C)*	*SWNTs density (μm^{-2})*
$P2VP_{79}$-*co*-$P(St\text{-}FI)_{347}$ (**5a**)	8300	151 530	1.55	360	88	25
$P2VP_{140}$-*co*-$P(St\text{-}FI)_{15}$ (**5b**)	14 700	6550	1.33	435	105	0
$P(St\text{-}FI)_{300}$ (**7**)	—	119 000	1.43	305	83	16
$P2VP_{146}$	15 300	—	1.02	—	97	0
$P(StFI)_{29}$	—	10 000	1.02	—	80	0

Abbreviations: GPC, gel permeation chromatography; PDI, polydispersity index; SWNTs, single-wall carbon nanotubes.
[a]M_n and PDI which are characterized by GPC and eluent with toluene.
[b]10 weight% loss temperature measured by thermal gravimetric analyzer under N_2.

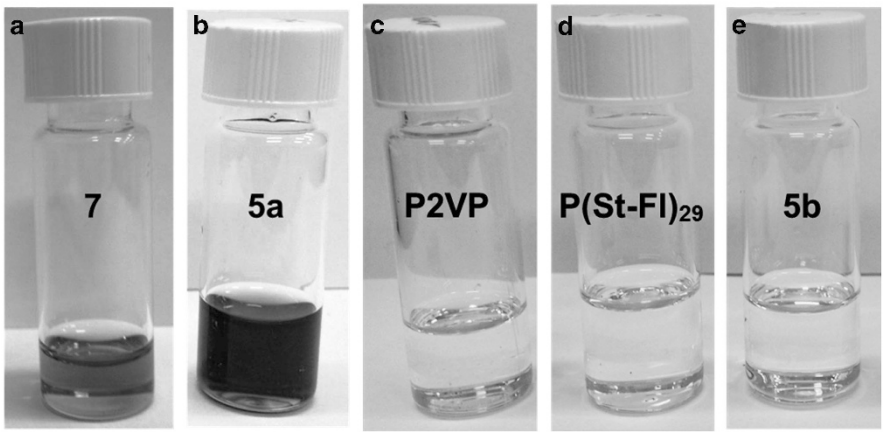

Figure 3 Dispersions of single-wall carbon nanotubes (SWNTs) in polymeric solutions: (**a**) P2VP, (**b**) $P(St\text{-}FI)_{29}$, (**c**) **5b**, (**d**) **7** and (**e**) **5a** after removing bundled SWNTs through centrifugation. A full color version of this figure is available at the *Polymer Journal* online.

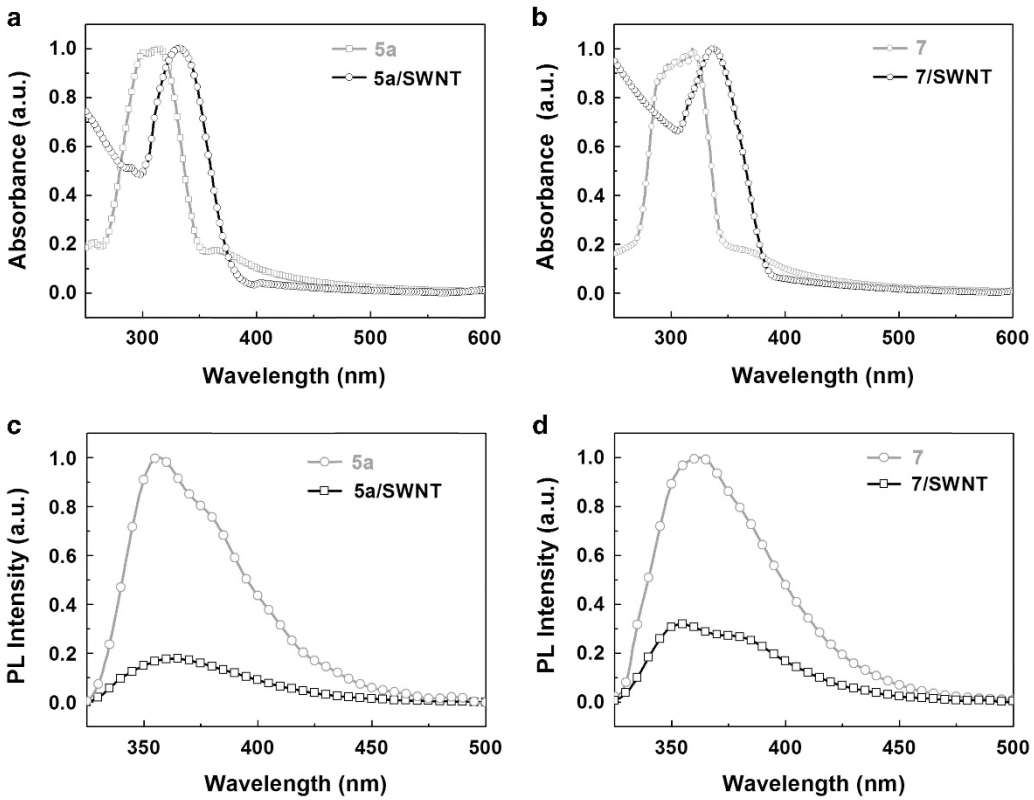

Figure 4 UV–vis spectra of (**a**) **5a** and **5a**/single-wall carbon nanotubes (SWNT) and (**b**) **7** and **7**/SWNT films on glass substrates. Photoluminescence (PL) spectra of (**c**) **5a** and **5a**/SWNT and (**d**) **7** and **7**/SWNT films on glass substrates. A full color version of this figure is available at the *Polymer Journal* online.

wrapping capability of P2VP is mainly due to the weak π–π interaction between 2-vinylpyridine segments and SWNTs. $P(St\text{-}Fl)_{29}$ and **5b**, both containing lower-molecular-weight pendant fluorene polymer blocks (M_n <10 000), also produce colorless solutions. This result is attributed to the short segment of the fluorene-containing pendant polymers weakly wrapping the surfaces of the SWNT and the removal of the bundled/aggregated SWNTs after the centrifugation process. However, the wrapping numbers of the SWNTs by **7** significantly increased for higher molecular weight ($M_n = 119\,000$ g mol^{-1}), and the color of mixture changed from colorless to light brown. This result indicates that the molecular weight of the polymer with the pendant conjugated moiety significantly affects the absorbed SWNTs. To demonstrate the feasibility of the hypothesized copolymer wrapping approach, a pendant fluorene-based copolymer **5a** with nearly the same pendant fluorene length ($M_n = 151\,530$ g mol^{-1}) relative to that of **7** and short flexible P2VP blocks was prepared. We determined that **5a** has a better dispersing ability for SWNTs than **7** and presents a dark brown color in the solution state, suggesting that the P2VP segment provides improved solubility to the exfoliated nanotubes by producing a steric barrier and repulsion interaction between the wrapped SWNTs. These **5a**/SWNTs dispersions also exhibited good stability for at least 1 month.

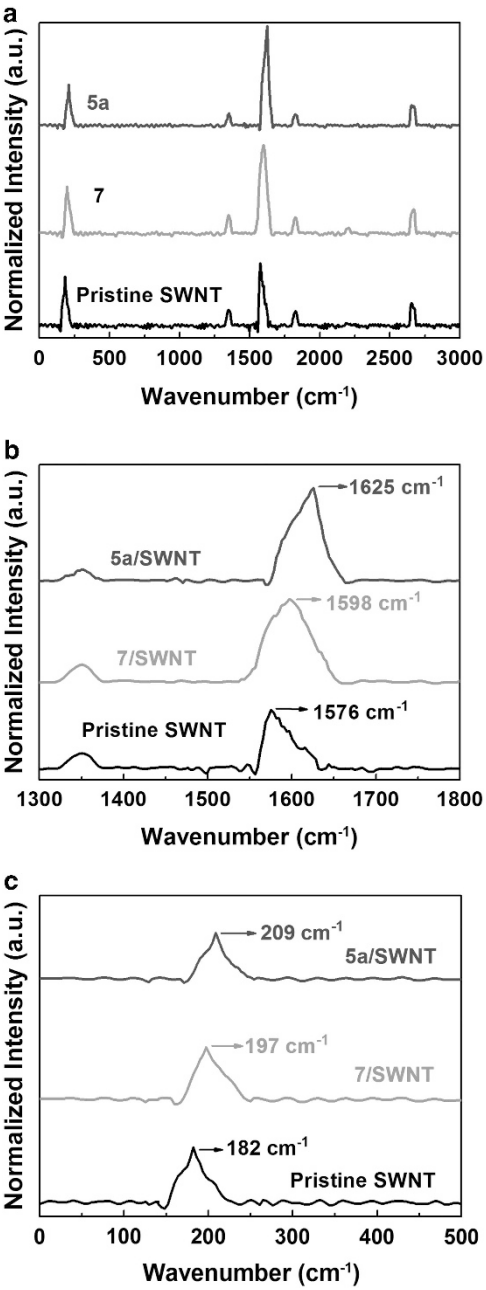

Figure 5 (**a**) Raman spectra of single-wall carbon nanotubes (SWNTs) dispersed with copolymers **5a** and **7** in toluene. The corresponding G and radical breathing modes (RBM) regions are depicted in (**b**) and (**c**). A full color version of this figure is available at the *Polymer Journal* online.

The selective dispersion of SWNTs wrapped in pendant polymers can be further investigated by UV–vis absorption and PL emission spectroscopy, as shown in Figure 4. A red-shift and broadening of absorption band in **5a**/SWNTs (Figure 4a) and **7**/SWNTs (Figure 4b) relative that in pure polymers is observed, indicating that the pendant polymers with increasingly π-conjugated moieties favor stronger π–π interactions with individual SWNTs.[30] Moreover, polymers **5a** and **7** exhibit a strong PL emission at 357 nm, whereas 82 and 68% decreases in PL intensity are observed on the addition of SWNTs to polymers **5a** (Figure 4c) and **7** (Figure 4d), respectively, clearly indicating that the PL quenching can be attributed to the expansion of a delocalized π-electron system among the side-chain fluorene moieties and SWNTs.[44] Raman spectroscopy was also used to characterize the electronic structure of the SWNTs before and after interaction with the **5a** copolymer and 7 homopolymer (Figure 5a). The G band of the SWNTs shifts to significantly higher frequency, from 1576 to 1625 and 1598 cm^{-1} (Figure 5b), and the radical breathing modes shift slightly from 182 to 209 and 197 cm^{-1} (Figure 5c) after dispersion with **5a** and **7**, respectively. The observed band shift here also suggests that a molecular-level interaction occurred between the SWNTs and the pendant copolymers.[30]

SWNT network formation

Previous reports have suggested that amines preferentially interact with SWNTs.[45] By depositing the nanotubes from solution onto surfaces functionalized with specified organic molecules using a dynamic spin assembly, the SWNTs could be separated with fairly high efficiency. Therefore, amine-terminated substrates were prepared using 3-aminopropyltriethoxysilane (surface contact angles of ~60°) for deposition of the polymer/SWNT composite film. After high-temperature annealing, the density of the SWNTs was further characterized by using AFM to evaluate the wrapping power of $P2VP_{79}$-*co*-$P(St\text{-}Fl)_{347}$ (**5a**) and $P(St\text{-}Fl)_{300}$ (**7**), as shown in Figure 6. AFM images were recorded at a minimum of four locations over the whole substrate (2.5×1.5 cm^2). Note that the average numbers of SWNT networks prepared from a 50 μl solution and spun at 4000 r.p.m. were determined over an area of 15×15 μm^2. All the polymers were completely removed at a high temperature >500 °C. The average diameter of the SWNTs determined from the AFM image is ~2 nm. When the same deposition conditions were applied to both **5a** and **7** polymer-wrapped SWNTs, densities of 25 and 16 SWNTs per μm^2 were achieved, respectively. It was found that the deviation of the SWNT density in the matrix was $< \pm 2\%$ for all substrates (four test samples), indicating good reproducibility of the pendant-polymer wrapping method. Moreover, the greater density of SWNTs wrapped by **5a** than SWNTs wrapped by **7** suggests that the P2VP segments act as a flexible spacer in a composite solution to effective disperse the SWNTs. This result is also consistent with the color change in polymer/SWNT composite solution and implies the importance of

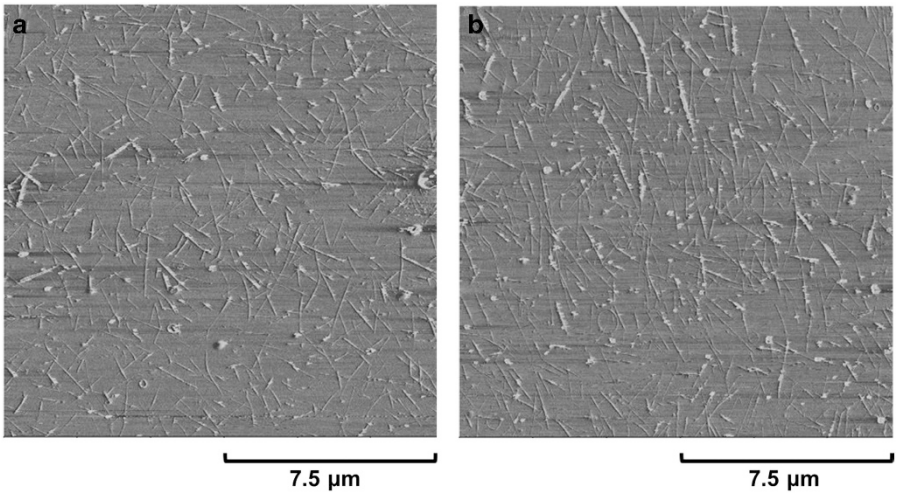

Figure 6 AFM images of polymer/single-wall carbon nanotubes (SWNT; 3:1) network after annealing at 500 °C on the amine-terminated modified SiO_2 surface in the case of (**a**) **7** and (**b**) **5a**. A full color version of this figure is available at the *Polymer Journal* online.

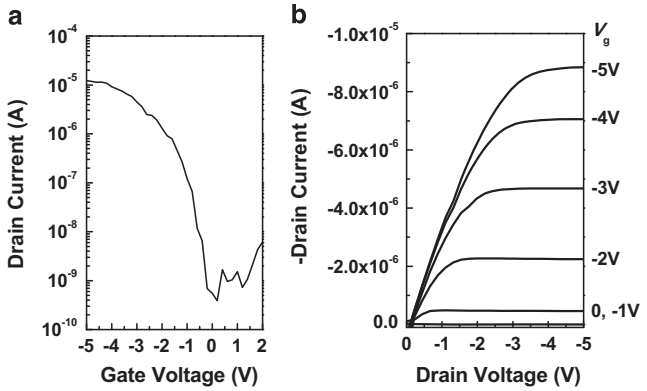

Figure 7 (**a**) Transfer and (**b**) output curves of single-wall carbon nanotubes (SWNT) random network field-effect transistor (FET).

the polymer block length and its structural composition to the total number of wrapped SWNTs.

Electrical properties of SWNT FET

It has been reported that electronic properties are heavily influenced by SWNT density.[46] The optimized SWNT density range for semiconducting channel was ~14–18 SWNTs per μm^2, which exhibited a high ON/OFF ratio and semiconductor properties.[46] However, the mobility steadily increased as the density increased beyond 18 SWNTs per μm^2. This result means that as the SWNT density reaches a critical point, the interconnections become dense enough the SWNTs network starts to exhibit conductor-like rather than semiconductor-like film behavior. The spraying deposition technique has been reported as an inexpensive, mass, and easy-scalable manufacturing process.[47,48] As a result, we used a spray-coating method to fabricate the uniform film, and the four-point probe resistance measurement was used to directly measure the resistance of SWNTs on the glass substrate. A schematic diagram of the experimental setup to deposit the polymer/SWNT composite via spray-coating is depicted in Figure 1. The nozzle-to-substrate surface distance is typically maintained at 10 cm. To avoid the polymers and residues affecting the electrical properties, high annealing temperatures up to 500 ºC are applied. In addition, the morphological properties of the spray-coated SWNTs network were investigated in $10 \times 10\ \mu m^2$ AFM images, as shown in Supplementary Figure S8. The films cover the substrate surface with a uniformly distributed random SWNT network. The SWNTs prepared by **5a** wrapping show a low sheet resistance of $220\ \Omega\ sq^{-1}$, which is comparable to those produced by using other methods (for example, vacuum filtration,[46] $160\ \Omega\ sq^{-1}$; lengthy sonication and centrifugation,[49] $85\ \Omega\ sq^{-1}$). However, the spray-coated SWNTs prepared from $P(St\text{-}Fl)_{300}$ (**7**) wrapping show a much higher resistance ($2720\ \Omega\ sq^{-1}$) due to the relatively poor wrapping power of this polymer in solution. This result indeed demonstrates the denser interconnection of SWNTs obtained from the greater wrapping power of $P2VP_{79}$-*co*-$P(St\text{-}Fl)_{347}$ (**5a**) enables the onset of conductivity, in which a critical SWNTs density is reached to form conductive pathways. Based on the above, strategies based on pendant-polymer-wrapped SWNTs represent an efficient approach because they allow sorting of the electrically metallic and semiconducting SWNTs, conditions required for FET applications. Thus, SWNTs wrapped by **5a** after annealing can be selected for use as a gate electrode, whereas spin-coated SWNTs wrapped by **7** can be used as a semiconductor for the FET channel. A top-contact bottom-gate FET was produced by thermally evaporating gold electrodes on top of the semiconducting SWNT networks. Figures 7a and b depict the transfer and output characteristics of the SWNT FET, respectively. The transfer characteristics (drain current (I_d) vs gate voltage (V_g)) of the prepared SWNT-based FET were measured with a fixed drain voltage (V_d) of -5 V and a gate voltage sweep from 2 to -5 V with a V_g step of 0.05 V. The output curves were characterized with a gate bias that varied from 0 to -5 V in steps of -1 V and exhibited well-defined linear and saturated regimes with a typical p-channel operation mode. Therefore, the fabricated SWNTs FET exhibit an average saturated mobility of $0.82\ cm^2\ V^{-1}\ s^{-1}$, a threshold voltage ($V_{th}$) of 0.35 V and an ON/OFF ratio of 2.8×10^4. It should be noted that the effective μ is determined by calculating the slope of $I_d^{1/2}$ versus V_g, where the exact length (L) of the electrodes and the estimated width (W) based on the numbers of SWNTs in contact with the electrode are applied. The subtle variations in device-to-device performance may result from slight variations in SWNT density in each batch during fabrication. In addition, the semiconducting layer of FET spin-coated from wrapped SWNTs by **5a** solution exhibits an extremely low ON/OFF ratio (or high OFF current) in Supplementary Figure S9, which implies

once again that a conductive pathway is formed because the polymer wrapping power has an important role in determining the electrical percolation threshold.

CONCLUSION

In summary, a simple and versatile approach to SWNT dispersion has been developed using copolymers with pendant conjugated fluorene moieties. The pendant conjugated fluorene segments can strongly bind to the SWNT surfaces through π–π interactions, while the P2VP block provides the flexibility for further increasing the solubility. Moreover, copolymers with a higher P(StFl) block ratio can disperse the SWNTs more efficiently. The approach based on polymer-wrapped SWNTs was used to fabricate FET devices, specifically the conducting electrode and semiconducting channel. In our work, the combinational spray-coated SWNTs at higher density (produced by **5a** wrapping) as a gate electrode and spin-coated SWNTs at lower density (produced by **7** wrapping) as a semiconductor layer resulted in a SWNT-based FET with a μ of 0.82 $cm^2 V^{-1} s^{-1}$, a V_{th} of 0.35 V and an ON/OFF ratio of 2.8×10^4. The present study demonstrates powerful solution-phase processing of polymer/SWNT composites to achieve debundling and good-quality dispersion of the SWNTs that is scalable and applicable to future transparent electronics.

CONFLICT OF INTEREST

The authors declare no conflict of interest.

ACKNOWLEDGEMENTS

The authors acknowledge final support from Ministry of Science and Technology (MOST) of Taiwan.

1 Baughman, R. H., Zakhidov, A. A. & de Heer, W.A. Carbon nanotubes - the route toward applications. *Science* **297**, 787–792 (2002).
2 Popov, V. N. Carbon nanotubes: properties and application. *Mater. Sci. Eng. R* **43**, 61–102 (2004).
3 Hu, L., Hecht, D. S. & Gruener, G. Carbon nanotube thin films: fabrication, properties, and applications. *Chem. Rev.* **110**, 5790–5844 (2010).
4 De Volder, M. F. L., Tawfick, S. H., Baughman, R. H. & Hart, A. J. Carbon nanotubes: present and future commercial applications. *Science* **339**, 535–539 (2013).
5 Avouris, P., Chen, Z. & Perebeinos, V. Carbon-based electronics. *Nat. Nanotechnol.* **2**, 605–615 (2007).
6 Avouris, P., Freitag, M. & Perebeinos, V. Carbon-nanotube photonics and optoelectronics. *Nat. Photon.* **2**, 341–350 (2008).
7 Cao, Q., Kim, H.-S., Pimparkar, N., Kulkarni, J. P., Wang, C., Shim, M., Roy, K., Alam, M. A. & Rogers, J. A. Medium-scale carbon nanotube thin-film integrated circuits on flexible plastic substrates. *Nature* **454**, 495–500 (2008).
8 Kauffman, D. R. & Star, A. Carbon nanotube gas and vapor sensors. *Angew. Chem. Int. Ed.* **47**, 6550–6570 (2008).
9 Snow, E. S., Perkins, F. K., Houser, E. J., Badescu, S. C. & Reinecke, T. L. Chemical detection with a single-walled carbon nanotube capacitor. *Science* **307**, 1942–1945 (2005).
10 Allen, B. L., Kichambare, P. D. & Star, A. Carbon nanotube field-effect-transistor-based biosensors. *Adv. Mater.* **19**, 1439–1451 (2007).
11 Hersam, M. C. Progress towards monodisperse single-walled carbon nanotubes. *Nat. Nanotechnol.* **3**, 387–394 (2008).
12 Komatsu, N. & Wang, F. A comprehensive review on separation methods and techniques for single-walled carbon nanotubes. *Materials* **3**, 3818–3844 (2010).
13 Huang, Y. Y. & Terentjev, E. M. Dispersion of carbon nanotubes: mixing, sonication, stabilization, and composite properties. *Polymers* **4**, 275–295 (2012).
14 Samanta, S. K., Fritsch, M., Scherf, U., Gomulya, W., Bisri, S. Z. & Loi, M. A. Conjugated polymer-assisted dispersion of single-wall carbon nanotubes: the power of polymer wrapping. *Acc. Chem. Res.* **47**, 2446–2456 (2014).
15 Nish, A., Hwang, J.-Y., Doig, J. & Nicholas, R. J. Highly selective dispersion of singlewalled carbon nanotubes using aromatic polymers. *Nat. Nanotechnol.* **2**, 640–646 (2007).
16 Byrne, M. T. & Gun'ko, Y. K. Recent advances in research on carbon nanotube-polymer composites. *Adv. Mater.* **22**, 1672–1688 (2010).
17 Star, A., Stoddart, J. F., Steuerman, D., Diehl, M., Boukai, A., Wong, E. W., Yang, X., Chung, S.-W., Choi, H. & Heath, J. R. Preparation and properties of polymer-wrapped single-walled carbon nanotubes. *Angew. Chem. Int. Ed.* **40**, 1721–1725 (2001).
18 Dalton, A. B., Stephan, C., Coleman, J. N., McCarthy, B., Ajayan, P. M., Lefrant, S., Bernier, P., Blau, W. J. & Byrne, H. J. Selective interaction of a semiconjugated organic polymer with single-wall nanotubes. *J. Phys. Chem. B* **104**, 10012–10016 (2000).
19 Liu, J., Moo-Young, J., McInnis, M., Pasquinelli, M. A. & Zhai, L. Conjugated polymer assemblies on carbon nanotubes. *Macromolecules* **47**, 705–712 (2014).
20 Liyanage, L. S., Lee, H., Patil, N., Park, S., Mitra, S., Bao, Z. & Wong, H.-S. P. Wafer-scale fabrication and characterization of thin-film transistors with polythiophene-sorted semiconducting carbon nanotube networks. *ACS Nano* **6**, 451–458 (2012).
21 Lee, H. W., Yoon, Y., Park, S., Oh, J. H., Hong, S., Liyanage, L. S., Wang, H., Morishita, S., Patil, N., Park, Y. J., Park, J. J., Spakowitz, A., Galli, G., Gygi, F., Wong, P. H.-S., Tok, J. B.-H., Kim, J. M. & Bao, Z. Selective dispersion of high purity semiconducting single-walled carbon nanotubes with regioregular poly(3-alkylthiophene)s. *Nat. Commun.* **2**, 541 (2011).
22 Gomulya, W., Costanzo, G. D., de Carvalho, E. J., Bisri, S. Z., Derenskyi, V., Fritsch, M., Fröhlich, N., Allard, S., Gordiichuk, P., Herrmann, A., Marrink, S. J., dos Santos, M. C., Scherf, U. & Loi, M. A. Semiconducting single-walled carbon nanotubes on demand by polymer wrapping. *Adv. Mater.* **25**, 2948–2956 (2013).
23 Jakubka, F., Schie β1, S. P., Martin, S., Englert, J. M., Hauke, F., Hirsch, A. & Zaumseil, J. Effect of polymer molecular weight and solution parameters on selective dispersion of single-walled carbon nanotubes. *ACS Macro Lett.* **1**, 815–819 (2012).
24 Hwang, J.-Y., Nishi, A., Doig, J., Douven, S., Chen, C. W., Chen, L. C. & Nicholos, R. J. Polymer structure and solvent effects on the selective dispersion of single-walled carbon nanotubes. *J. Am. Chem. Soc.* **130**, 3543–3553 (2008).
25 Lo, C.-H., Tsai, M.-T., Liu, B. H., Isoda, S. & Ruan, J. Oriented association of multiwall carbon nanotubes upon efficient epitaxial organization of polyfluorene. *Carbon* **93**, 342–352 (2015).
26 Han, J., Ji, Q., Qiu, S., Li, H., Zhang, S., Jin, H. & Li, Q. A versatile approach to obtain a high-purity semiconducting single-walled carbon nanotube dispersion with conjugated polymers. *Chem. Commun.* **51**, 4712–4714 (2015).
27 Rice, N. A., Subrahmanyam, A. V., Coleman, B. R. & Adronov, A. Effect of induction on the dispersion of semiconducting and metallic single-walled carbon nanotubes using conjugated polymers. *Macromolecules* **48**, 5155–5161 (2015).
28 Liu, Y. Q., Yao, Z. L. & Adronov, A. Functionalization of single-walled carbon nanotubes with well-defined polymers by radical coupling. *Macromolecules* **38**, 1172–1179 (2005).
29 Zou, J., Khondaker, S. I., Huo, Q. & Zhai, L. A general strategy to disperse and functionalize carbon nanotubes using conjugated block copolymers. *Adv. Funct. Mater.* **19**, 479–483 (2009).
30 Zou, J., Liu, L., Chen, H., Khondaker, S. I., McCullough, R. D., Huo, Q. & Zhai, L. Dispersion of pristine carbon nanotubes using conjugated block copolymers. *Adv. Mater.* **20**, 2055–2060 (2008).
31 Hwang, S. K., Choi, J. R., Bae, I., Hwang, I., Cho, S. M., Huh, J. & Park, C. High-temperature operating non-volatile memory of printable single-wall carbon nanotubes self-assembled with a conjugate block copolymer. *Small* **9**, 831–837 (2013).
32 Kwak, M., Gao, J., Prusty, D. K., Musser, A. J., Markov, V. A., Tombros, N., Stuart, M. C., Browne, W. R., Boekema, E. J., ten Brinke, G., Jonkman, H. T., van Wees, B. J., Loi, M. A. & Herrmann, A. DNA Block copolymer doing it all: from selection to self-assembly of semiconducting carbon nanotubes. *Angew. Chem. Int. Ed.* **50**, 3206–3210 (2011).
33 Sung, J., Huh, J., Choi, J.-H., Kang, S. J., Choi, Y. S., Lee, G. T., Cho, J., Myoung, J.-M. & Park, C. Ultrathin electronic composite sheets of metallic/semiconducting carbon nanotubes embedded in conjugated block copolymers. *Adv. Funct. Mater.* **20**, 4305–4313 (2010).
34 Petrov, P., Stassin, F., Pagnoulle, C. & Jerome, R. Noncovalent functionalization of multi-walled carbon nanotubes by pyrene containing polymers. *Chem. Commun.* 2904–2905 (2003).
35 Yuan, W. Z., Sun, J. Z., Dong, Y., Hai, Häussler M., Yang, F., Xu, H. P., Qin, A., Lam, J. W., Zheng, Q. & Tang, B. Z. Wrapping carbon nanotubes in pyrene-containing poly (phenylacetylene) chains: solubility, stability, light emission, and surface photovoltaic properties. *Macromolecules* **39**, 8011–8020 (2006).
36 Yuan, W. Z., Mao, Y., Zhao, H., Sun, J. Z., Xu, H. P., Jin, J. K., Zheng, Q. & Tang, B. Z. Electronic interactions and polymer effect in the functionalization and solvation of carbon nanotubes by pyrene- and ferrocene-containing poly(1-alkyne)s. *Macromolecules* **41**, 701–707 (2008).
37 Lou, X., Daussin, R., Cuenot, S., Duwez, A.-S., Pagnoulle, C., Detrembleur, C., Bailly, C. & Jérôme, R. Synthesis of pyrene-containing polymers and noncovalent sidewall functionalization of multiwalled carbon nanotubes. *Chem. Mater.* **16**, 4005–4011 (2004).
38 Fujigaya, T. & Nakashima, N. Methodology for homogeneous dispersion of single-walled carbon nanotubes by physical modification. *Polym. J.* **40**, 577–589 (2008).
39 Tuncel, D. Non-covalent interactions between carbon nanotubes and conjugated polymers. *Nanoscale* **3**, 3545–3554 (2011).
40 Bilalis, P., Katsigiannopoulos, D., Avgeropoulos, A. & Sakellariou, G. Non-covalent functionalization of carbon nanotubes with polymers. *RSC Adv.* **4**, 2911–2934 (2014).
41 Sugiyama, K., Hirao, A., Hsu, J.-C., Tung, Y.-C. & Chen, W.-C. Living anionic polymerization of styrene derivatives para-substituted with pi-conjugated oligo(fluorene) moieties. *Macromolecules* **42**, 4053–4062 (2009).
42 Hsu, J.-C., Sugiyama, K., Chiu, Y.-C., Hirao, A. & Chen, W.-C. Synthesis of new star-shaped polymers with styrene-fluorene conjugated moieties and their multicolor luminescent ordered microporous films. *Macromolecules* **43**, 7151–7158 (2010).
43 Zhang, D., Ryu, K., Liu, X., Polikarpov, E., Ly, J., Tompson, M. E. & Zhou, C. Transparent, conductive, and flexible carbon nanotube films and their application in organic light-emitting diodes. *Nano Lett.* **6**, 1880–1886 (2006).

44 Imit, M. & Adronov, A. Effect of side-chain halogenation on the interactions of conjugated polymers with SWNTs. *Polym. Chem.* **6**, 4742–4748 (2015).
45 Chattopadhyay, D., Galeska, L. & Papadimitrakopoulos, F. A route for bulk separation of semiconducting from metallic single-wall carbon nanotubes. *J. Am. Chem. Soc.* **125**, 3370–3375 (2003).
46 LeMieux, M. C., Sok, S., Roberts, M. E., Opatkiewicz, J. P., Liu, D., Barman, S. N., Patil, N., Mitra, S. & Bao, Z. Solution assembly of organized carbon nanotube networks for thin-film transistors. *ACS Nano* **3**, 4089–4097 (2009).
47 Kang, B., Lee, W. H. & Cho, K. Recent advances in organic transistor printing processes. *ACS Appl. Mater. Interfaces* **5**, 2302–2315 (2013).
48 Diao, Y., Shaw, L., Bao, Z. & Mannsfeld, S. C. B. Morphology control strategies for solution-processed organic semiconductor thin films. *Energy Environ. Sci.* **7**, 2145–2159 (2014).
49 Yim, J. H., Kim, Y. S., Koh, K. H. & Lee, S. Fabrication of transparent single wall carbon nanotube films with low sheet resistance. *J. Vac. Sci. Technol. B* **26**, 851–855 (2008).

Supplementary Information accompanies the paper on Polymer Journal website (http://www.nature.com/pj)